International Journal of Material Forming (2019) 12:331–353
https://doi.org/10.1007/s12289-018-1419-2

ORIGINAL RESEARCH

Influence of machining parameters on surface quality during high speed edge trimming of carbon fiber reinforced polymers

Mohamed Slamani[1,2] · Jean-François Chatelain[1] · Hossein Hamedanianpour[1]

Received: 19 February 2018 / Accepted: 7 May 2018 / Published online: 14 June 2018

Abstract
CVD diamond-coated carbide tools could provide an economical alternative for trimming CFRPs components compared to their PCD tools counterpart. Nevertheless, there are still some technical issues to understand related to wear resistance and surface quality. In this work, a CVD tool with six straight flutes was used to investigate the relationship between surface roughness, surface damage, tool wear, cutting force and cutting parameters during the high speed trimming of CFRPs. Statistical techniques for identifying and selecting the best cutting conditions for CVD tool are developed. In terms of tool wear, results show that the best operational condition to minimize the tool wear is achieved at lower feed rates and higher cutting speeds. Experimental results show also that a 0° ply orientation represents the worst case and produces the maximum tool wear. Furthermore, a strong correlation between the feed force and the tool wear was observed. It was found that the surface roughness decreases as a reciprocal function of cutting length. This decrease was due to the matrix burning/sticking and the thermal damage related to the low thermal conductivity of CFRP. In such situation, R_a becomes inappropriate indicator for roughness evaluation. On the other hand, it wasn't seen any type of delamination or fiber pull-out on the trimmed surface of all coupons for the three tool life tests. Accordingly, delamination can be avoided using high fixture rigidity, high quality of CFRP laminates, a suitable cutting tool and stable operational conditions.

Keywords Surface roughness · Surface quality · Tool wear · Cutting force · Regression model · Carbon fiber reinforced polymer (CFRP)

Introduction

Ever since Carbon fiber reinforced polymers (CFRPs) were invented over 50 years ago, their use has continued to increase considerably, especially in aerospace industries, thanks to their attractive properties, such as their strength to-weight ratio, damping capacity, durability, and extreme corrosion resistance.

Machining of CFRPs is different from and more complicated than that of conventional metals and their alloys due to the high abrasiveness of the carbon fibers and the heat sensitivity of CFRP, which makes them difficult to machine. Further detailed discussions on machining of composite materials may be found in [1–6].

The chip formation mechanism is different when machining CFRPs from when metals are machined; a compression shearing or fracture of the fiber reinforcement and matrix occur in CFRP machining, while a plastic deformation takes place in metal cutting. The shearing and fracture of the fibers and matrix of CFRPs generally produce powder like chips or dust, rather than uniform chips [7, 8]. The chip formation mechanism requires a sharp tool with a large positive rake angle. The hardness and toughness of the cutting tool are necessary to overcome the abrasiveness of the fibers and the loads which are produced when fibers fracture. Only a limited range of tool materials satisfy these conditions. Normally, with an increase in hardness, the toughness decreases and vice versa [2, 7].

✉ Mohamed Slamani
mohamed.slamani@polymtl.ca

[1] Mechanical Engineering Department, École de Technologie Supérieure, Montreal, Canada

[2] Mechanical Engineering Department, Faculty of Technology, University of M'sila, M'sila, Algeria

Fig. 1 HURON K2X8 CNC machine used for the experiments

Cutting forces play a crucial role in machinability assessment as well as on the quality of machined parts. Due to the inhomogeneous nature of CFRPs, cutting forces are fluctuating and periodic. The periodicity is due to the fact that the cutting tool cuts the fibers and the matrix phases alternatively, which in turn leads to different magnitudes for the cutting forces magnitudes during machining. The periodicity can also due to the changes of fiber angles relative to the speed. Many research studies show that cutting forces are influenced by many factors, such as cutting conditions, the geometry of the cutting tool and the properties of the material to be machined [9–11]. Chatelain et al. [11] studied the effect of tool geometry on cutting force, delamination and roughness during the trimming of multilayered CFRP laminates. Initially, some experiments were carried out using three Carbide CVD coating cutting tools with different geometries at different cutting conditions. Their results show that the cross-cut geometry produces the highest axial component of the cutting force and the worst surface integrity. More recently, an interesting approach to adaptive fractal analyses of cutting force signals during trimming of CFRP was presented by Rimpault et al. [12]. To describe the signal complexities variations, they performed Fractal analyses on the measured signals of the cutting forces. They found that their developed approach applied on the cutting force signals can be used successfully to estimate the surface quality and the tool wear during trimming of CFRP.

Haiyan et al. [13] studied cutting forces during the helical milling of CFRPs. They established a relationship between cutting parameters, tool wear and cutting forces. Furthermore they formulated and used a mechanistic cutting force model to predict cutting forces during the helical milling of CFRP. They showed a good agreement between the predicted and the measured cutting forces (maximum error was 18%).

Boudelier et al. [14] proposed an analytical model for predicting the cutting force during trimming of CFRP laminate using diamond abrasive cutters. Hence a continuous model of tool engagement is proposed. The validity of their model is verified on multidirectional CFRP laminate for different fibres orientation and widths of cut. They claimed that their model allows accurate prediction of cutting forces over the entire range studied.

The main tool wear mechanism in the trimming of FRPs is abrasion due to the interrupt nature of milling. When the cutting tool has an insufficient toughness and weak cutting edges, microfracture and chipping becomes significant problems. In the milling of CFRPs, special tool material properties, such as resistance to abrasive wear and high fracture toughness, are important. For a cutting tool, it is also essential to have high thermal conductivity as well, because the heat generated in cutting zone is conducted to the cutting tool. Tool materials meeting these criteria are fine-grained cemented carbides, PCD and diamond-coated carbides.

A CVD diamond-coated carbide tool with six straight flutes was used by Slamani et al. [15] during high speed CNC trimming of CFRPs. Two models have been assessed to predict tool wear and cutting force. Compared to the multiplicative model, they found that the exponential model was more accurate.

Xu and Zhang [16] studied the tool wear mechanism during cutting of fibre-reinforced polymer composites.

Fig. 2 CVD coated cutting tool

Table 1 Tool geometry and specifications

No. of teeth	Rake	Relief	Helix	Length of cut [mm]	Overall length [mm]	Tool type	Diameter
6	8°	10°	10°	25.4	76.2	Coated carbide	9.525

They found that tool wear significantly affect the material removal mechanisms and surface integrity of the machined composites. It was found also that the introduction of ultrasonic vibration to the cutting tool can drastically reduce its wear rate.

High reliability of CFRP components depends generally upon the quality of the machined surface. However, due to the inhomogeneity and the anisotropic nature of CFRP the machined surface is usually rough and less regular compared to conventional metals [5]. Surface quality depends on the tool geometry, the dynamics of the machining process, cutting conditions (cutting velocity and feed rate), workpiece material characteristics, fiber type, fiber orientation, matrix type and work piece/machine rigidities. Temperature generated during machining process has also an effect on the surface quality [17]. Regarding rigidity, proper clamping is very important in the machining of CFRPs because it directly affects surface roughness and induces vibration. Surface integrity is related to the physical and chemical conditions of the surface layer after machining including fiber pullout, fiber breakage, delamination, matrix removal, burning and decomposition. Because the reliability of machined components depends on the surface finish quality, it is therefore essential to both qualify and quantify the surface finish.

Ghidossi et al. [18] verified the cutting effects on the surface roughness and surface damage of three types of polymer matrix composite coupons. They confirmed that for composite materials, surface roughness is not an appropriate indicator for damage. In terms of surface quality and delamination, they found that there was a big difference between when specimens were machined with worn tools and with new ones.

Rajasekaran et al. [19] verified the effect of machining parameters on surface roughness during the turning of CFRP using carbide cutting. A fuzzy model was developed and used to predict the surface roughness of the machined component. It was shown that there was a good correlation between the proposed model and the experimental data. In addition, based on experimental results, it was found that the feed rate was the important parameter affecting the surface roughness, meaning that with an increase in the feed rate, the surface roughness increases.

\The fiber orientation of the CFRPs plays an important role in the chip formation mechanism as well as the quality of the machined components. Arola et al. [20] found that with 0° fiber orientations, chip formation involved failure along the fiber-matrix interface through bending and fracture perpendicular to the fiber. Wang et al. [21] found that fiber orientation was a main factor affecting the surface integrity of a machined component. In their study, the 90° orientation was a critical angle, meaning that over 90°, an intense subsurface damage occurs.

More recently (2017), another study carried out by Wang et al. [22] showed that during orthogonal milling of unidirectional CFRP laminates, surface cavities occur and lead to significant surface damage. They found also that surface cavities are not influenced by the cutting parameters (speed and feed) and are the main factors affecting the surface roughness (R_a). In order to improve the surface quality and reduce the occurrence of cavities in the machined CFRP parts, inclination milling was adopted. They indicated that the proposed strategy improve the surface roughness (R_a) and the surface quality significantly.

To recap, numerous studies have been conducted to investigate the damage caused during machining of CFRPs [16, 23, 24]. However, the number of studies on trimming is quite limited. Furthermore, the relationship between tool wear, surface roughness and surface damage during the trimming of CFRPs has not been well investigated. This

Table 2 Process parameters (two factors and three levels)

Process parameters	Level		
	Low	Medium	High
Cutting velocity (m/min)	200	300	400
Feed (mm/min)	1524	2794	4064

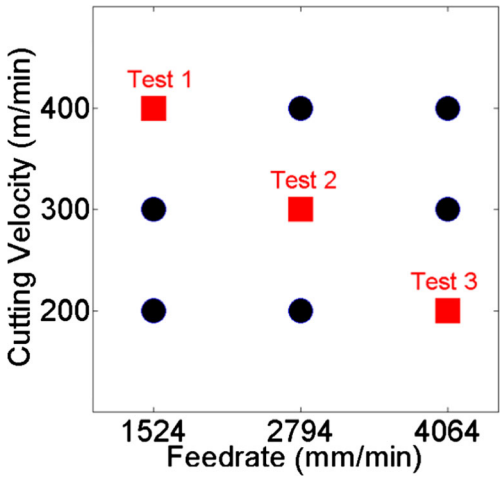

Fig. 3 A full factorial design of experiments (3^2 trials)

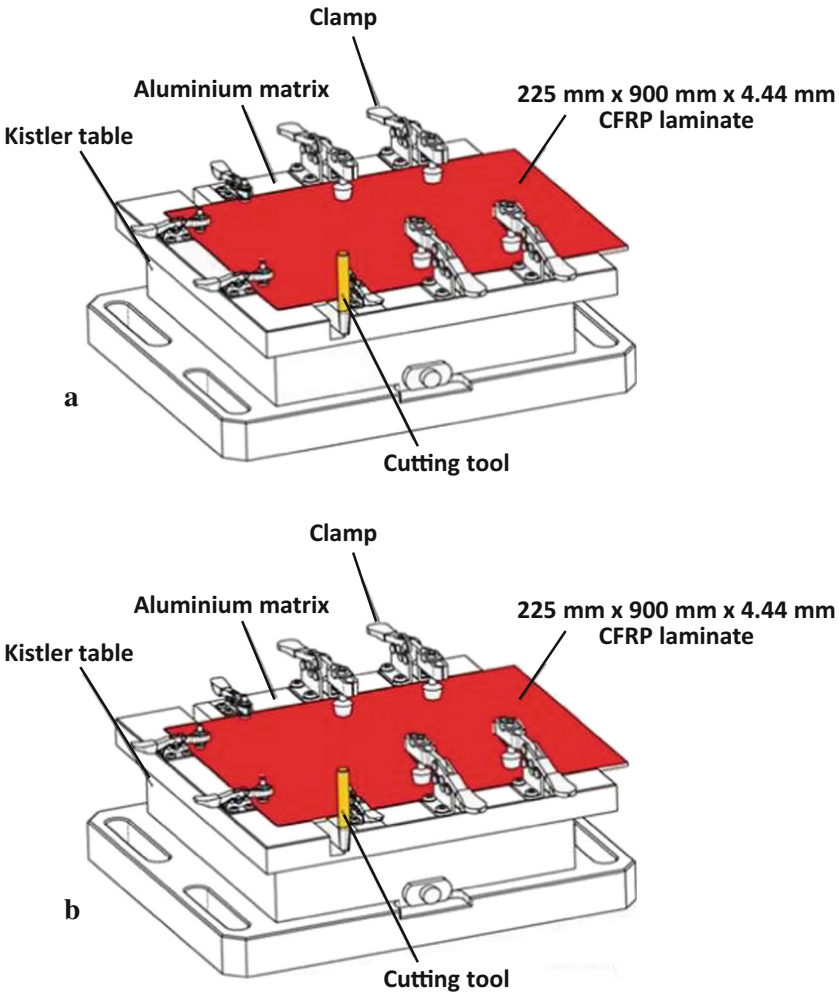

Fig. 4 Experimental set-up: (**a**) short run trimming, (**b**) long run trimming

phenomenon remains poorly understood qualitatively and models for surface roughness prediction are needed. Moreover, unlike many research projects, which base their studies on the machining of unidirectional laminates, our research considers a multilayer quasi-isotropic material utilized in the aerospace industry.

On the other hand, PCD tools are extremely hard, which is a key characteristic for successfully machining CFRPs [11]. However, PCD tools geometry is very limited and their cost is comparatively quite high compared to their CVD tools counterpart. Furthermore, the unit cost of a PCD tool ranges from 3 to 5 times the unit cost of a competitive CVD diamond coated carbide tool [25]. Another advantage of the CVD tools is that they offers the flexibility of different cutter geometries and the chemically inert properties of diamond do not react with composite resins during machining [25]. This work thus focuses mainly on analyzing the tool wear behavior, evaluation of surface damage, providing an understanding of the machinability of CFRPs using a CVD diamond coated carbide tool and developing empirical models for predicting surface roughness and the cutting force during the high speed trimming of quasi-isotropic CFRP laminates used in the aerospace filed. The contribution of each cutting parameter on surface roughness and the cutting force was analyzed by means of an analysis of variance.

Materials and methods

In order to study the influence of the tool wear and the cutting condition on surface quality, machining tests were conducted by trimming CFRP specimens under different cutting conditions using a 3-axis high speed machining center HURON K2X10 (Fig. 1) and a CVD diamond-coated carbide tool with six straight flutes (Fig. 2). The specifications and the geometry of the cutting tool are shown in Table 1.

The investigated material was an autoclave-cured 24-ply CFRP laminate with stacking sequence [90°, −45°, 45°, 0°, 45°, −45°, 45°, −45°, 0°, −45°, 45°, 90°]s. The fiber volume fractions of the tested CFRP were 64% and the finale total thickness of the laminate was 4.44 mm.

Because CFRPs machining is dusty, messy and harmful, the dust must be frequently vacuumed. During these trimming tests a dust extraction system was used as shown in Fig. 1.

In this work, a full factorial design of experiments (DOE) for two factors ($k = 2$) and three levels yielded 9 trials (3^k) were designed and carried out. The two main factors influencing process performance and selected in this work were cutting velocity and feed rate. For each factor, three levels are considered (low, medium and high) as shown in Table. 2. The nine cutting velocity-feed combinations are shown in Fig. 3. For each combination, the three cutting force components were measured and analyzed.

According to the results of the nine cutting velocity and feed rate combinations (Fig. 3), three tests were selected in order to carry out the tool life tests and surface quality assessment. The three selected combinations (cutting velocity and feed rate) are presented by squares in Fig. 3.

The experiments described in this work were conducted in order to achieve two goals. The first goal was to generate tool wear as function of distance for different cutting conditions, and the second goal was to assess the surface roughness of the machined CFRP specimens as a function of the cutting conditions and tool wear. To accomplish this, two experimental set-up were developed to properly fixe the specimens during

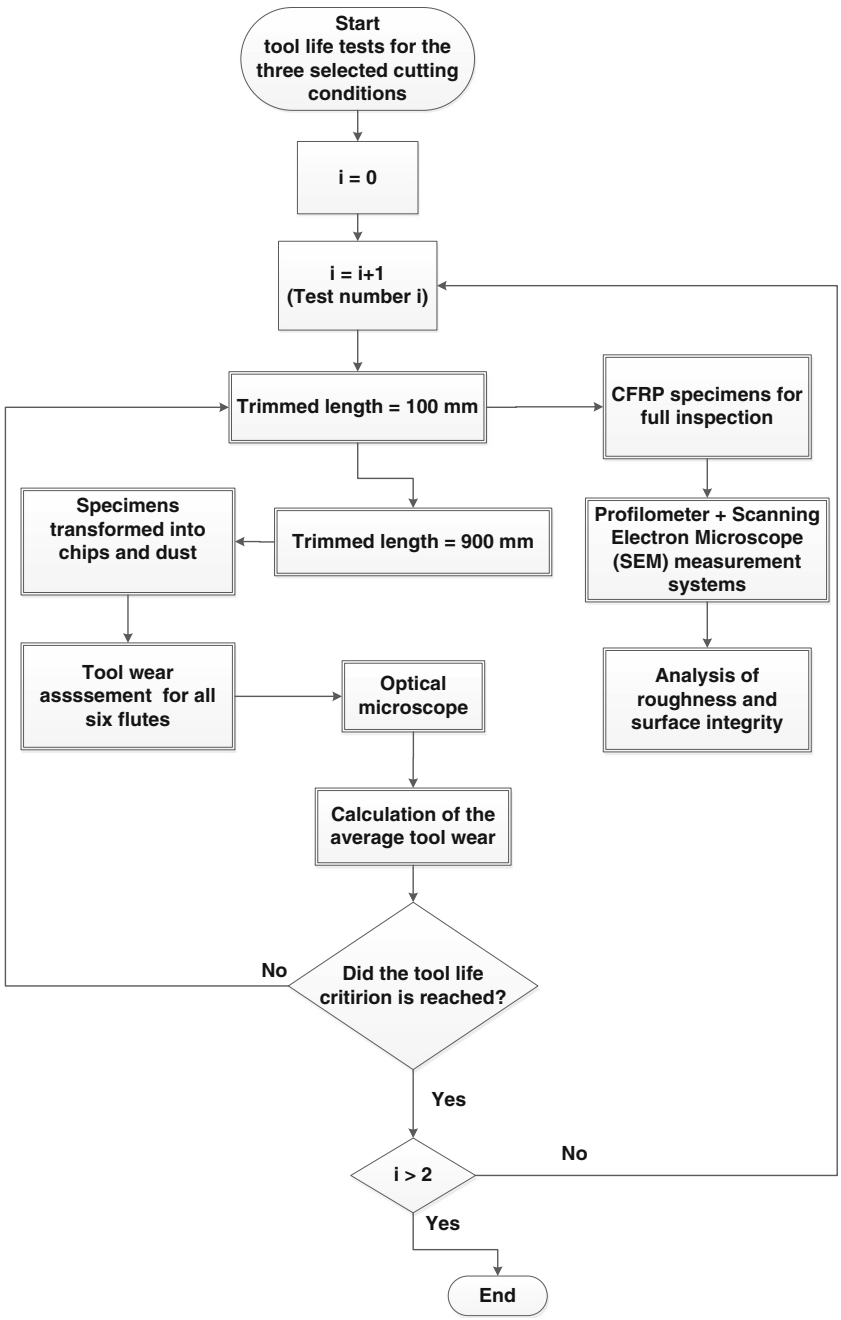

Fig. 5 Flow chart of the tool life tests for the three selected cutting conditions

Fig. 6 Optical microscope type Keyence VHX-600 + 500F

trimming. As illustrated in Fig. 4, one machining fixture was used for the short run trimming (100 mm of length) and the other was used for the long run trimming (900 mm of length). As shown in the flaw chart presented in the Fig. 5, the test is realized through an iterative process until the tool wear reached the flank wear criterion (average flank wear reached 0.3 mm), i.e. in each tool life experiment, the cutting tool trimmed 100 mm with a short run trimming, and then 900 mm with a long run trimming.

Furthermore, before each short run test, the cutting tool wear was measured with an optical type Keyence VHC-600 + 500F microscope (Figs. 6 and 7).

In this test, and according to the ISO 8688–2 standard [26], the tool life failure was 0.3 mm for average maximum flank wear (Fig. 7).

The surface damage was inspected using a scanning electron microscope type Hitachi S-3600 N (Fig. 8), whereas, the surface roughness was measured using a profilometer type Mitutoyo SURFPAK SJ-400 (Fig. 9).

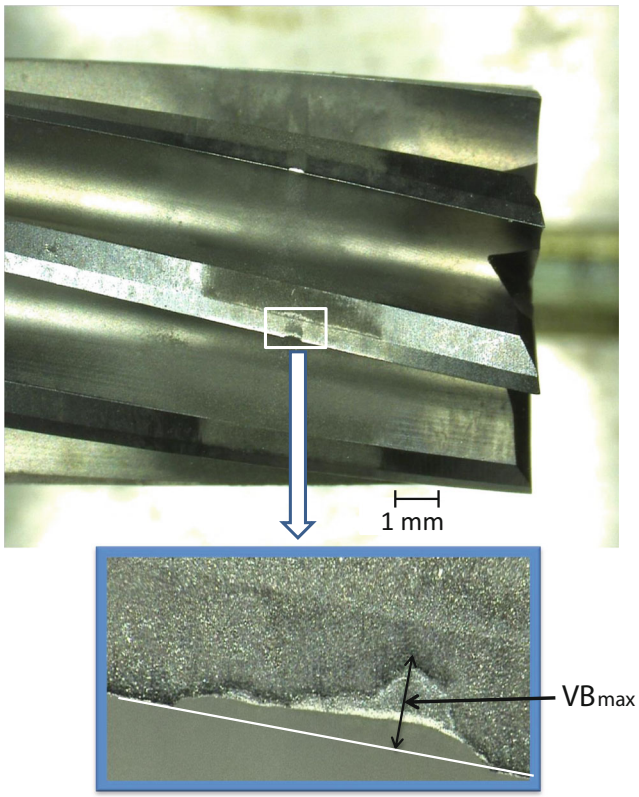

Fig. 7 Measurement of tool wear (VBmax)

Results and discussion

Results of the nine preliminary tests

In each experiment, cutting forces components in the x-, y- and z-directions were measured using a 3-axis dynamometer table (type Kistler 9255B), as shown in Fig. 1, then, Fast Fourier Transform (FFT) technique was applied for each measured signal. Results show that the measured signals of the three cutting force components for all of the nine combination of cutting velocity-feed were harmonic (Fig. 10). The harmonics of the tooth passing frequency and the spindle speeds were not superposed; this meant that the FFT spectrum of the cutting force components did not show the presence of amplification at measuring devise resonance.

Analysis of variance (ANOVA) is one of the most commonly used statistical approaches to determine what factors and combination of factors that significantly affect the response. In this work, the combined effects of the cutting velocity and feed rate on the cutting forces components and surface roughness parameters are investigated using ANOVA technique at significant level of 5% ($\propto = 0.05$). Tables 3, 4, and 5 show the ANOVA and F test results related to cutting forces components. It can be seen from these tables that the most significant factor influencing the normal cutting force and axial cutting force is the feed rate (f) with percentage contributions of 85.58 and 78.71% respectively. The next significant factor is the interaction between the cutting velocity (V_C) and the feed rate (f) with percentage contributions of 11.21 and 20.84% respectively. The effect of the cutting velocity is found almost negligible with contribution of 3.21 and 0.44% respectively.

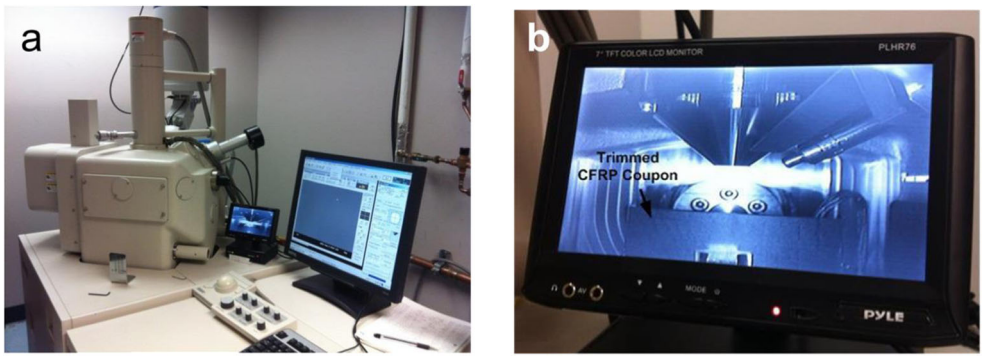

Fig. 8 Measurement of the surface damage, **a**) SEM-type Hitachi S-3600 N, **b**) CFRP laminate in the vacuum chamber of SEM

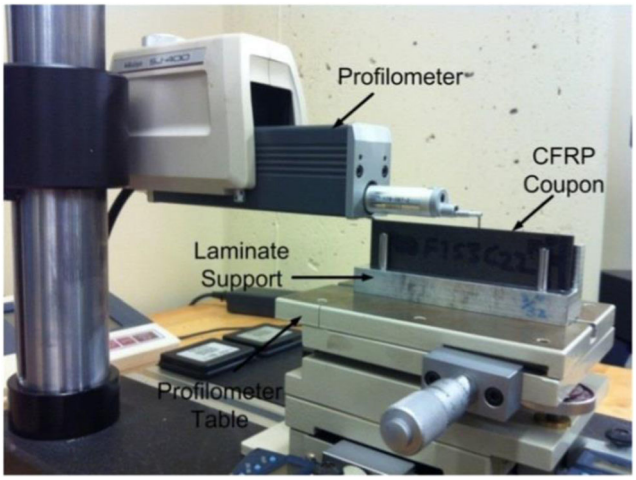

Fig. 9 Profilometer Mitutoyo type SJ 400 SURFPAK

Based on the ANOVA test the estimated regression models for the normal cutting force and the axial cutting force are shown in Eqs. (1) and (2) respectively:

$$\hat{F}_N = 71 + 82.87 \times 10^{-3} \times f - 153.83 \times 10^{-3} \times V_C - 9.641 \times 0^{-5} \times f \times V_C \quad (1)$$

$$\hat{F}_a = -4.55 - 19.03 \times 10^{-3} \times f + 13.66 \times 10^{-3} \times V_C + 3.15 \times 10^{-5} \times f \times V_C \quad (2)$$

Concerning the feed force, ANOVA analysis illustrated in Table 5 shows that the interaction effect of the cutting velocity-feed has the highest statistical significance (50.90%) followed by the cutting velocity (33.20%) and feed rate (15.9%).

The estimated model is presented in Eq. (3).

$$\hat{F}_f = -213.88 + 32.15 \times 10^{-3} \times f + 445.33 \times 10^{-3} \times V_C - 18.50 \times 10^{-5} \times f \times V_C \quad (3)$$

Figure 11 shows the measured versus predicted values of the cutting force components using Eq. 1–3. The calculated R squares show that the estimated models explain about of 99%, 97 and 91% the variability in the response variables for the normal, axial and feed cutting forces respectively.

Tables 6, 7, and 8 present ANOVA results for surface roughness R_a, R_t and R_z respectively. It is observed from these

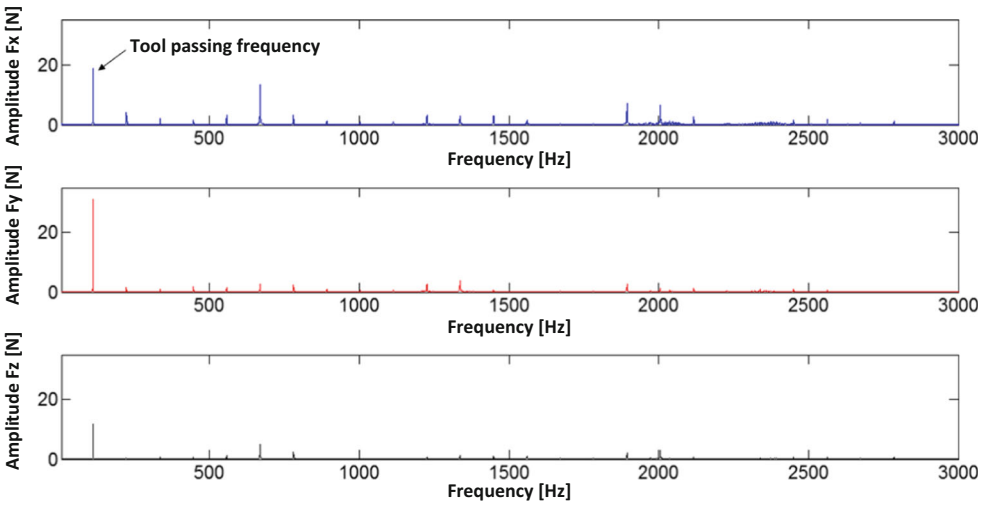

Fig. 10 FFT results in the ninth preliminary test in x-, y-, and z-directions

Table 3 Analysis of variance (ANOVA) of response variables for normal force

Source	Parameter estimate	Standard error	F-value	Percentage; cont. %
Intercept	71	27.09		
Feed rate (f)	82.87×10^{-3}	9.10×10^{-3}	83.10	85.58
Cutting velocity (V_C)	-153.83×10^{-3}	87.14×10^{-3}	3.12	3.21
Interaction ($f \times V_C$)	-9.64×10^{-5}	2.92×10^{-5}	10.88	11.21

tables that the interaction effect of the cutting velocity and feed rate has the highest contribution (74.50%, 68.07 and 75.27% respectively). The next significant parameters for the R_a *and* R_t is the cutting velocity (25.25 and 17.35% respectively). The contribution of the feed rate on R_t was 14.58%, whereas its effect on R_a was found negligible (0.25%) . The effect of the feed rate on the R_v was found more important than the cutting velocity effects with contribution of 21.13 and 3.60% respectively.

The regression equations for the R_a, R_t *and* R_v are:

$$\hat{R}_a = 2.58 - 0.09 \times 10^{-3} \times f + 8.72 \times 10^{-3} \times V_C + 0.5 \times 10^{-5} \times f \times V_C \quad (4)$$

$$\hat{R}_t = 59.96 - 6.4 \times 10^{-3} \times f - 66.84 \times 10^{-3} \times V_C + 4.44 \times 10^{-5} \times f \times V_C \quad (5)$$

$$\hat{R}_v = 22.35 - 3.38 \times 10^{-3} \times f - 13.37 \times 10^{-3} \times V_C + 2.05 \times 10^{-5} \times f \times V_C \quad (6)$$

Figure 12 illustrates the measured versus predicted values for the roughness parameters R_a, R_t *and* R_v. The coefficients of determination (R^2) were 0.82, 0.86 and 0.89 respectively.

Table 4 Analysis of variance (ANOVA) of response variables for axial force

Source	Parameter estimate	Standard error	F-value	Percentage; contr.%
Intercept	−4.55	9.95		
Feed rate (f)	-19.03×10^{-3}	3.34×10^{-3}	32.46	78.71
Cutting velocity (V_C)	13.66×10^{-3}	32.01×10^{-3}	0.18	0.44
Interaction ($f \times V_C$)	3.15×10^{-5}	1.07×10^{-5}	8.60	20.84

Table 5 Analysis of variance (ANOVA) of response variables for feed force

Source	Parameter estimate	Standard error	F-value	Percentage; cont. %
Intercept	−213.88	45.92		
Feed rate (f)	32.15×10^{-3}	15.41×10^{-3}	4.35	15.90
Cutting velocity (V_C)	445.33×10^{-3}	147.71×10^{-3}	9.09	33.20
Interaction ($f \times V_C$)	-18.50×10^{-5}	4.96×10^{-5}	13.94	50.90

Table 6 Analysis of variance (ANOVA) of response variables for R_a surface roughness

Source	Parameter estimate	Standard error	F-value	Percentage; cont. %
Intercept	2.58	5.55		
Feed rate (f)	-0.09×10^{-3}	1.86×10^{-3}	0.0024	0.25
Cutting velocity (V_C)	8.72×10^{-3}	17.84×10^{-3}	0.2390	25.25
Interaction ($f \times V_C$)	0.5×10^{-5}	0.6×10^{-5}	0.7045	74.50

Table 7 Analysis of variance (ANOVA) of response variables for R_t surface roughness

Source	Parameter estimate	Standard error	F-value	Percentage; cont. %
Intercept	59.96	18.45		
Feed rate (f)	-6.4×10^{-3}	6.19×10^{-3}	1.0656	14.58
Cutting velocity (V_C)	-66.84×10^{-3}	59.39×10^{-3}	1.2684	17.35
Interaction ($f \times V_C$)	4.44×10^{-5}	1.99×10^{-5}	4.9755	68.07

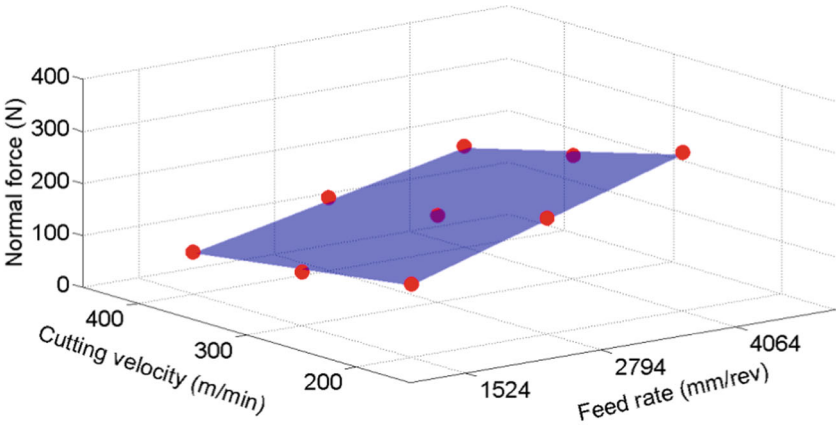

a) Normal cutting force

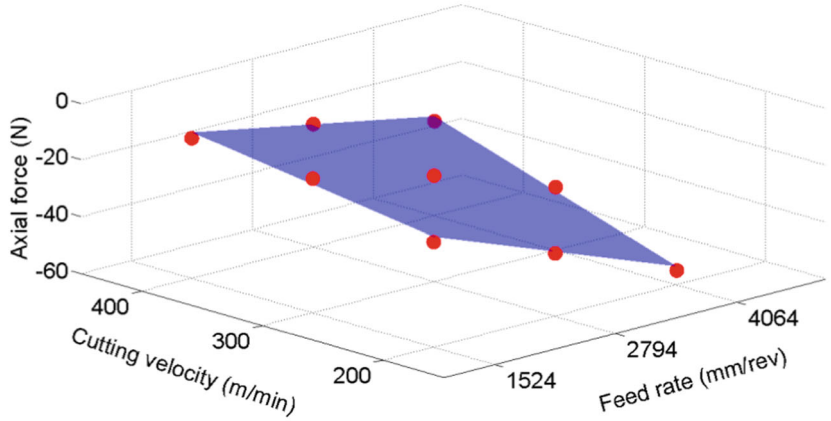

b) Axial cutting force

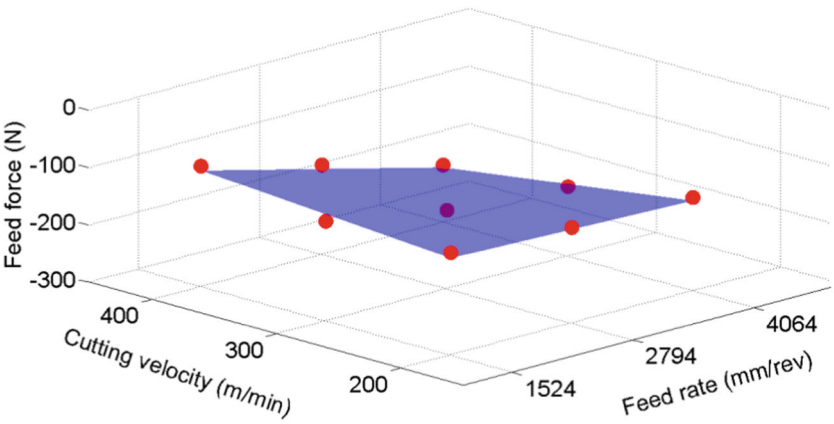

c) Feed cutting Force

Fig. 11 Measured versus predicted values of the cutting force components for the nine preliminary tests

Table 8 Analysis of variance (ANOVA) of response variables for R_v surface roughness

Source	Parameter estimate	Standard error	F-value	Percentage; cont. %
Intercept	22.35	8.51		
Feed rate (f)	-3.38×10^{-3}	2.85×10^{-3}	1.40	21.13
Cutting velocity (V_C)	-13.37×10^{-3}	27.37×10^{-3}	0.24	3.60
Interaction ($f \times V_C$)	2.05×10^{-5}	0.92×10^{-5}	4.98	75.27

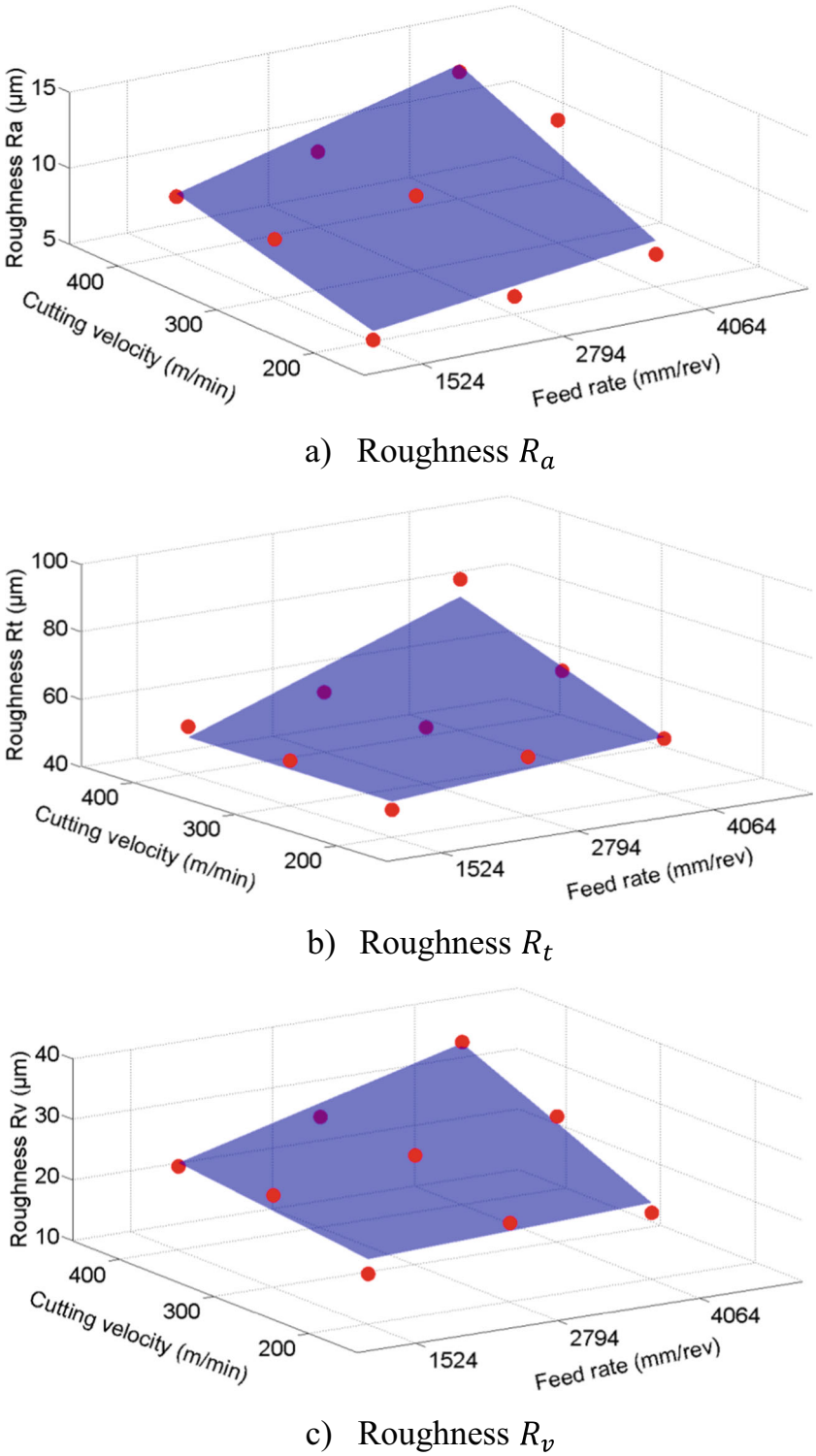

Fig. 12 Measured versus predicted values of the roughness parameters for the nine preliminary tests

Results of the three selected tests

Tool wear analysis

Figures 13, 14, and 15 show the tool wear progression on the flank face for tooth #5 during the three selected tests, respectively. As shown in these figures, as the cutting length increases, so does the tool wear. It could be assumed that, the cutting tool edges (flank faces) deteriorated with an increase in the distance (length of cut) in all three tool life tests.

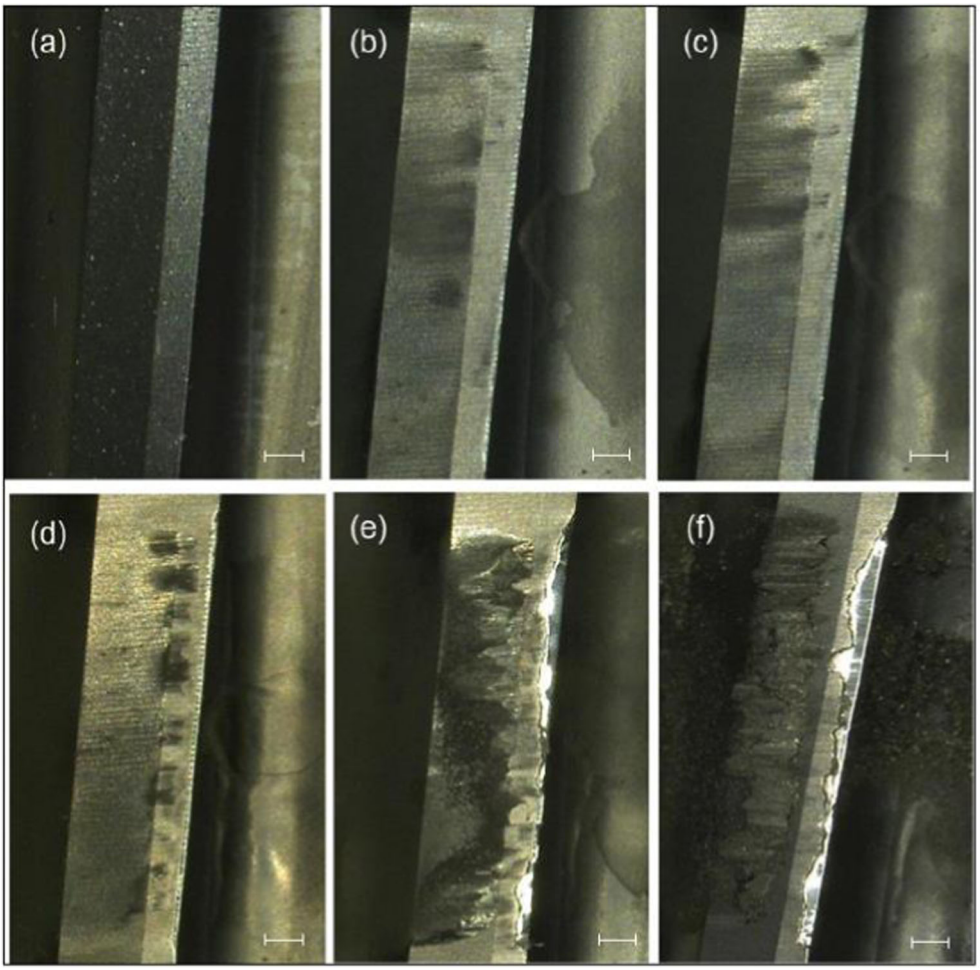

Fig. 13 Tool wear at **a**) 0, **b**) 4, **c**) 9, **d**) 15.8, **e**) 27.2, and **f**) 28.2 m of cut for Tooth#5 in Test 1 (each graduation corresponds to 500 μm)

Effect of fiber orientation on tool wear profile

It was observed from the optical microscope images presented in Fig. 16 that 0° ply orientation played an important role on the tool wear profile. For example, in both tests 2 and 3, the 16th ply (0° ply orientation) produced the maximum tool wear, while in test 1, it was the 9th ply (0° ply orientation) that generated the maximum tool wear. In the case of a 0° ply orientation, the feed rate and fiber orientation directions were same. It could be assumed that in this case, the tool-chip contact length increase, and that the increase most probably caused further tool wear.

Cutting forces analysis

During machining with six-tooth end mill, each tooth engaged and removed material while the chip thickness was not constant. The six flutes in one tool revolution produced six peaks, as shown in Fig. 17. In this Figure, each peak indicates the passage of one tooth. The amplitudes of the six peaks are not identical, and the differences between are most probably due to tool run-out.

Generally, the profiles of the cutting forces in the x-, y-, and z-directions are similar for different cutting conditions. These profiles present three different zones in the tool engagement process. Zone I corresponds to the immersion of the cutter into the workpiece. The cutting force starts to increase from a zero value in this zone. The cutter engagement brings high energy to the CFRP laminate, and this energy is immediately dissipated in the laminate. During zone I, the end mill cutter feeds into the workpiece, and when the end mill tool is fully engaged, the tool enters the next zone (zone II). Zone II is the steady state condition, which is categorized by a cyclical cutting force profile from one revolution to another with almost constant force amplitude. In zone III, the cutting forces start to change and attain their peak value. Here, the tool is disengaging from the workpiece, and consequently, the chip thickness decreases. This in turn causes a high vibration, which increases the cutting force. When the unsupported final part of the CFRP laminate is removed, the cutting force decreases

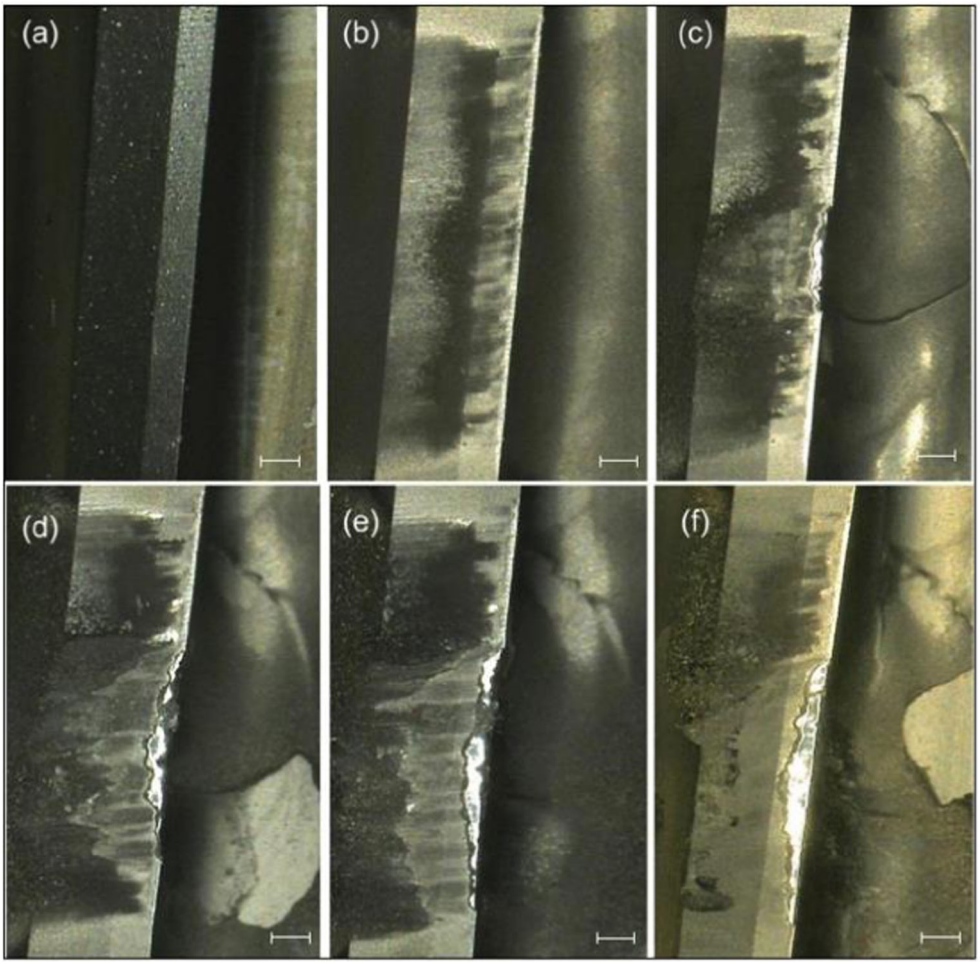

Fig. 14 Tool wear at **a**) 0, **b**) 4, **c**) 9, **d**) 12, **e**) 14 and **f**) 15 m of cut for Tooth #5 in Test 2 (each graduation corresponds to 500 μm)

smoothly. This decrease is most likely due to the decrease in chip thickness that occurs. The cutting force finally decreases to a zero value when there is no CFRP laminate left to remove [27]. The tool engagement process for the six-flute cutting tool is shown in Fig. 18.

Regarding the effect of tool wear on the cutting forces, the cutting forces in the x-, y-, and z-directions were compared at the beginning and at the end of each tool life test. Figures 19, 20, and 21 illustrate the recorded cutting forces in the x-, y-, and z-direction during trimming of the CFRP laminate using a new tool and a worn tool. Based on these figures, the feed forces, (F_y), at the end of the tool life test (using worn tool) were significantly higher than those at the beginning of the tool life test (using new tool). For example, in test 1, when the average too wear was zero (new tool), the average feed force was 95 N, while at the end of the tool life, when the average tool wear was 0.42 mm, the feed force was 519 N. This fact indicates that the feed forces increased due to the chipping of the cutting tool (worn tool). For the normal and axial forces (F_x*and* F_z), they did not increase significantly with an increase in tool wear, and were almost constant. On the other hand, the effect of the tool wear increase was obvious on the y components of the cutting forces (feed force). For the F_x (normal force) and F_z (axial force) components, the effect of the tool wear was not very significant.

Effect of cutting parameters and tool wear on cutting force

Figure 22 shows the evolution of the cutting force components as a function of the tool wear for three tool life tests. It can be seen from this figure that there is a weak correlation between the normal force and the tool wear (Fig. 22a). The computed correlation coefficient in this case was only 0.36. The axial force is also less affected by the tool wear (Fig. 22b). The

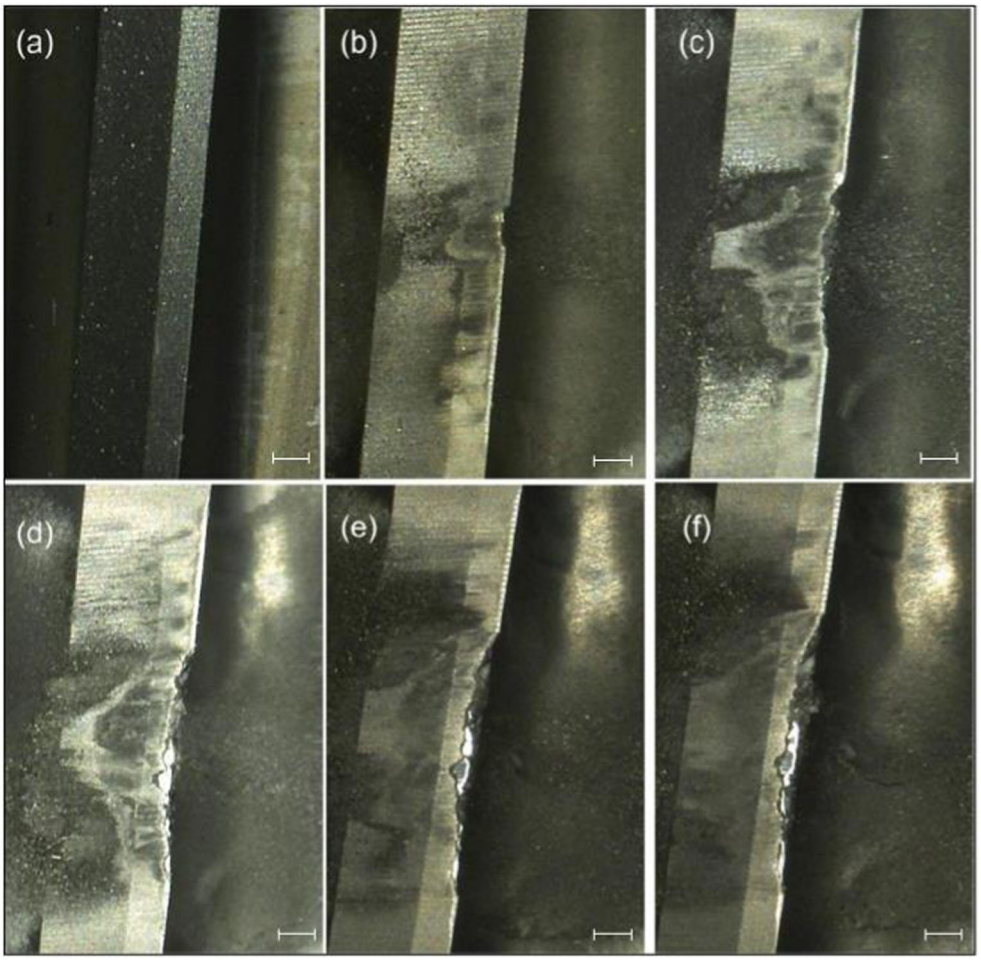

Fig. 15 Tool wear at **a**) 0, **b**) 4, **c**) 9, **d**) 14, **e**) 19 and **f**) 20 m of cut for Tooth #5 in Test 3 (each graduation corresponds to 500 μm)

computed correlation coefficient $\rho = -0.36$, indicate that there is a weak negative association between this two variables. Figure 22c shows that there is a strong relationship between the feed force and the tool wear. The computed correlation coefficient was −0.9, means that the two variables are almost totally inversely correlated.

Of the three tool life tests we conducted, the highest cutting force value was obtained in Test 2 ($V_C = 300$ *m/min* and $f = 2794$ *mm/min*), while the lowest cutting force value related to the lowest tool wear value was generated in Test 1 ($V_C = 400$ *m/min* and $f = 1524$ *mm/min*).

Effect of cutting parameters and tool wear on surface roughness

According to Slamani et al. [28] and Berube [29], the worst surface roughness during trimming operation of CFRP was on the −45° plies. Sheikh-Ahmed et al. [30] found also that the surface roughness in the transverse direction was mostly higher than that in the longitudinal direction. In this test, the surface roughness at −45° ply orientation was measured using longitudinal method over a distance of 14 mm (Fig. 23), with a Mitutoyo SJ-400 SURFPAK profilometer (Fig. 9), and the arithmetic average roughness parameter R_a was considered for surface roughness modeling and analysis. The cut-off value (the longest nominal wavelength) depends on the range of R_a. In this study, R_a was varied between 1 and 11 μm, therefore, the value of Lc Cut-off should be chosen 2.5 mm according to the ASME. ANSI B46.1standard [31].

The objective of this test is to assess the surface roughness of the machined specimens as a function of the cutting conditions and machining length ($R_a = f(V_C, f, L)$). As mentioned above (Fig. 5), the first specimen

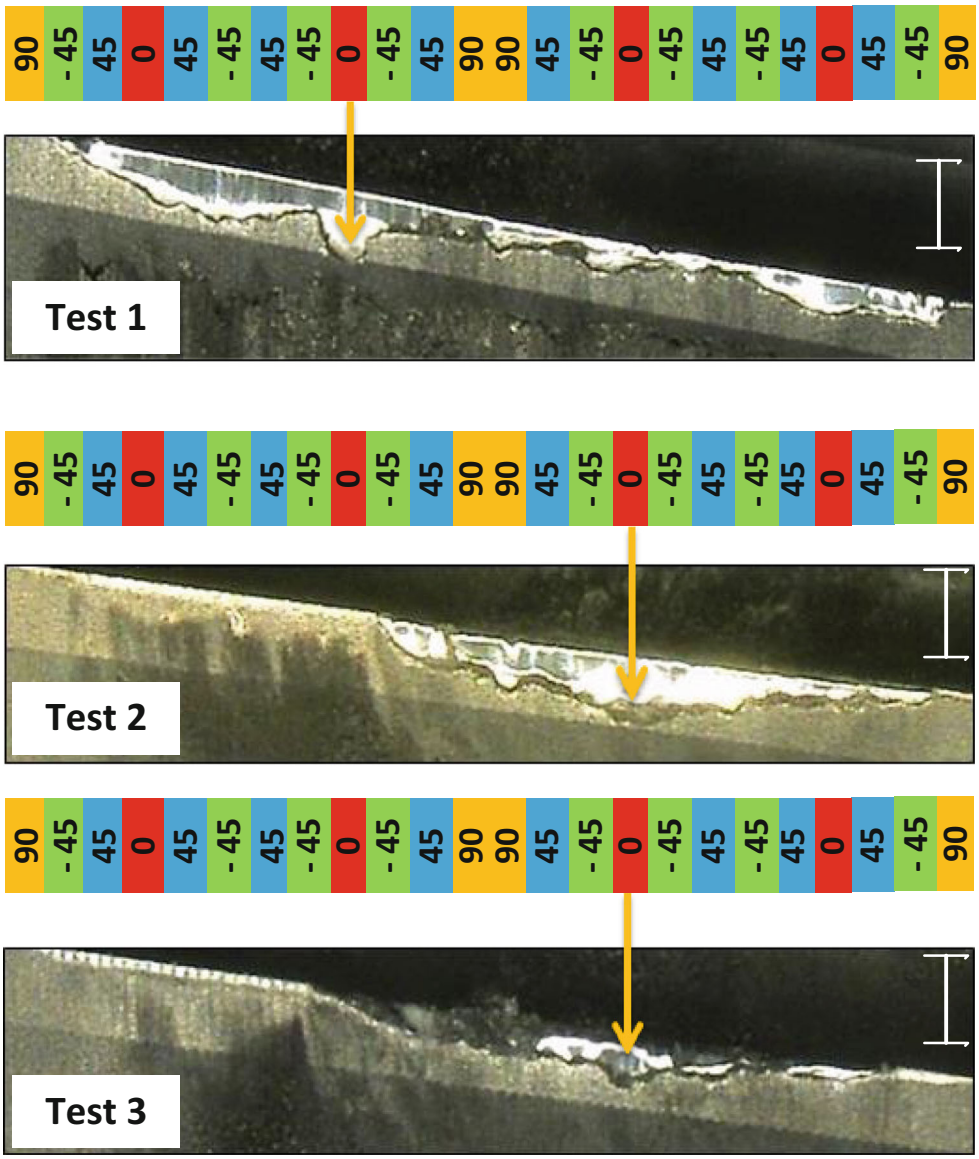

Fig. 16 Effect of fiber orientation on tool wear (each graduation corresponds to 500 μm)

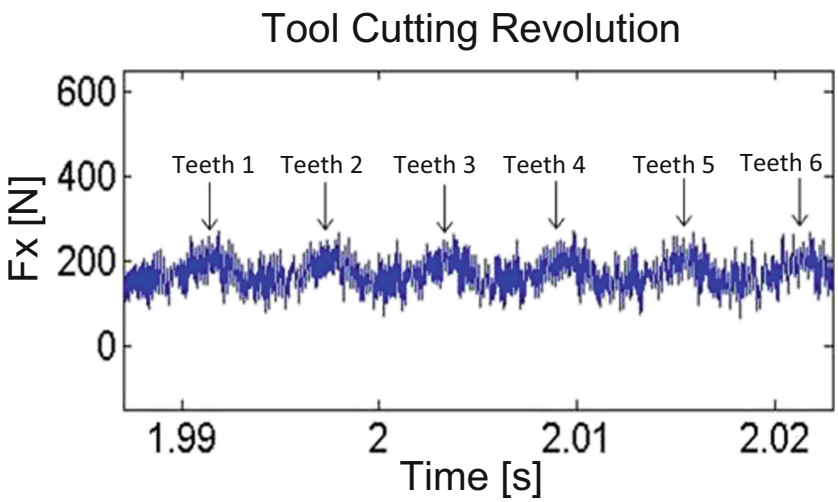

Fig. 17 One tool cutting revolution for new six-tooth end mill in Test 1

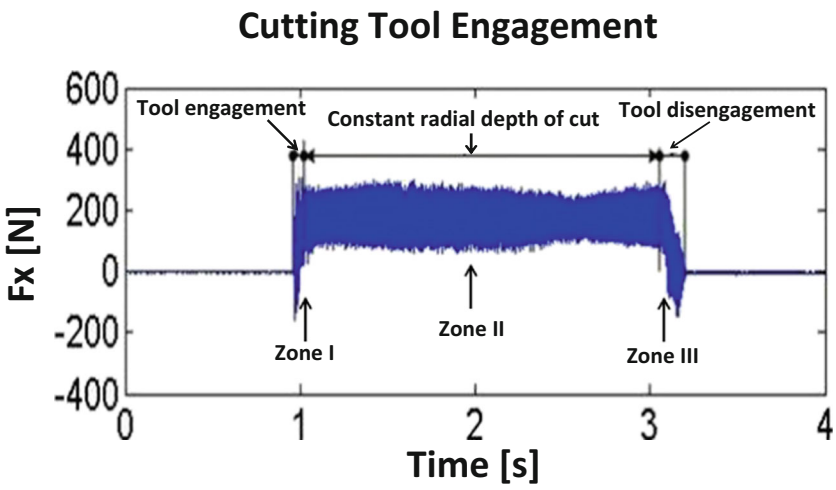

Fig. 18 Tool engagement process for new six-tooth end mill in Test 1

was measured immediately after the first short cut (first 100 mm trimmed length), then the surface roughness was measured after each 1 m trimming (900 mm as long cut +100 mm as short cut). The measured surface roughness for all of the three tests is presented in Fig. 24.

Figure 24 shows that in all tool life tests, the surface roughness (R_a) decreased with an increase in cutting length. This behavior goes against the effect of tool wear. This can be explained by the fact that the surface roughness was decreased due to the matrix burning/sticking and the breaking of the carbon fiber beneath the machined surface (using worm tool). This result is consistent with the other studies in the literature, confirming that R_a is inappropriate indicator for roughness evaluation [32, 33]. However, if R_a is considered the evaluation must be followed by SEM micrograph analysis to confirm the absence of surface damages.

The results presented in Fig. 24 show that the surface roughness decreases as a reciprocal function of cutting length. Accordingly, a reciprocal regression model could be more appropriate and effective than other models. In this work, a full second-order reciprocal regression model with a two-level interaction of the linear terms was fitted to the raw data.

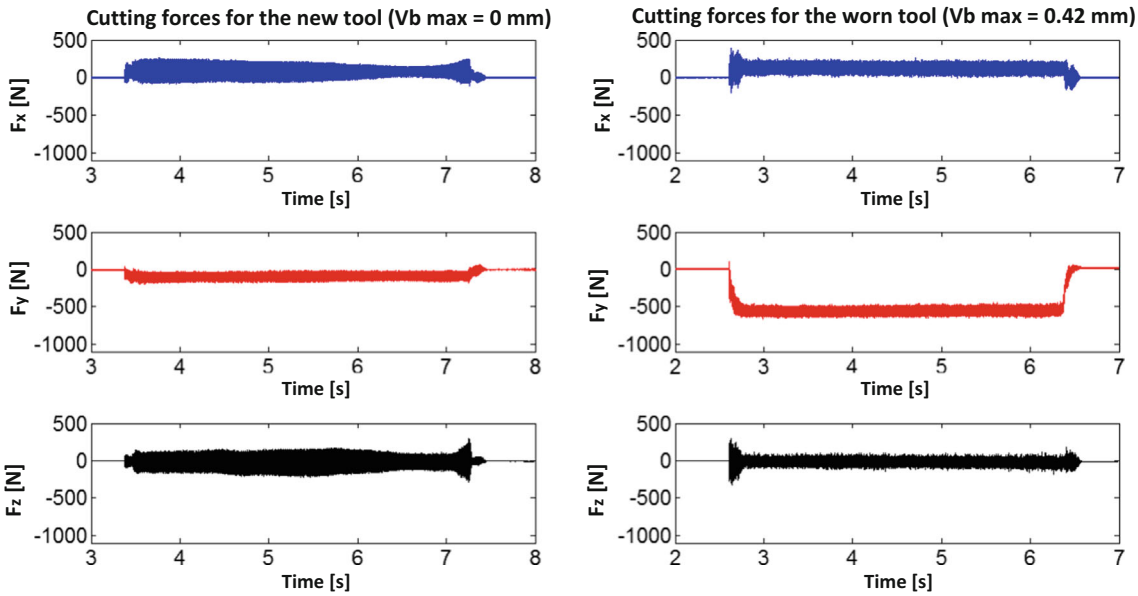

Fig. 19 Recorded forces in x-, y-, and z-directions using new and worn tools in Test 1

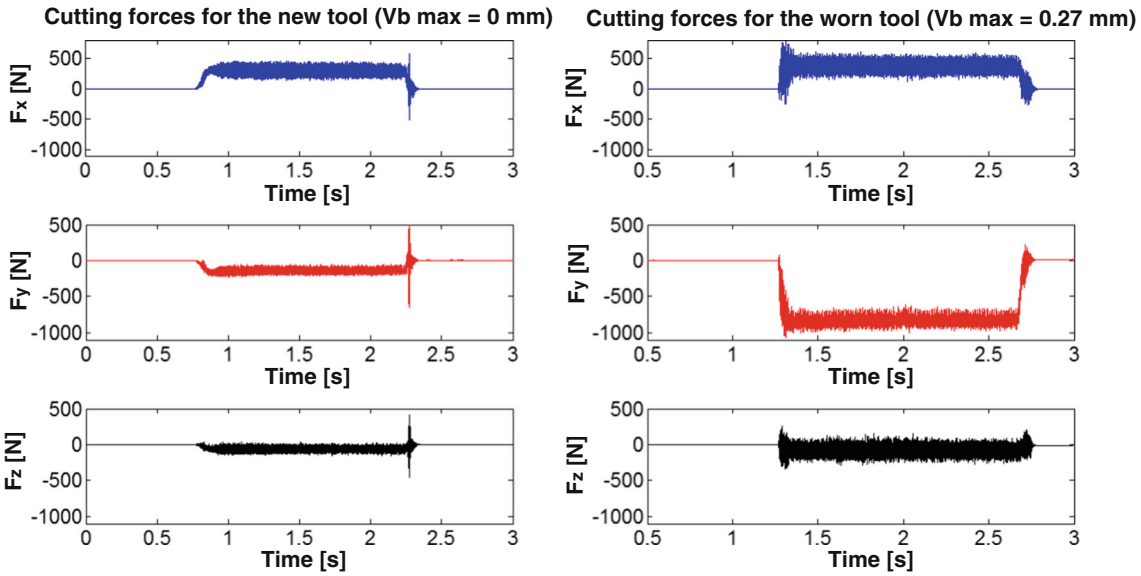

Fig. 21 Recorded forces in x-, y-, and z-directions using new and worn tools in Test 3

The regression equation is:

$$\hat{R}_a = \beta_0 + \frac{\beta_1}{L} + \frac{\beta_2}{f} + \frac{\beta_3}{V_C} + \frac{\beta_4}{L \times f} + \frac{\beta_5}{L \times V_C} + \frac{\beta_6}{f \times V_C} + \frac{\beta_7}{L^2} + \frac{\beta_8}{f^2} + \frac{\beta_9}{V_C^2} + \frac{\beta_{10}}{(L \times f)^2} + \frac{\beta_{11}}{(L \times V_C)^2} + \frac{\beta_{12}}{(f \times V_C)^2} + \varepsilon \quad (7)$$

where:

$\hat{R}_a$ is the estimated average surface roughness, f, V_C, L and ε are the feed rate, cutting velocity cutting length and random error, respectively.

The selection of the most significant variables is a very important process in regression it conditions the predictive capacity of the model. In this work, a parameter selection technique based on sensitivity analysis and backward stepwise regression was used. For the sensitivity analysis, singular value decomposition (SVD) tool was applied. SVD essentially provides a measure of sensitivity of unknown coefficients to perturbations [34]. Using this selection technique, the redundant parameters and the variable with the smallest contribution were

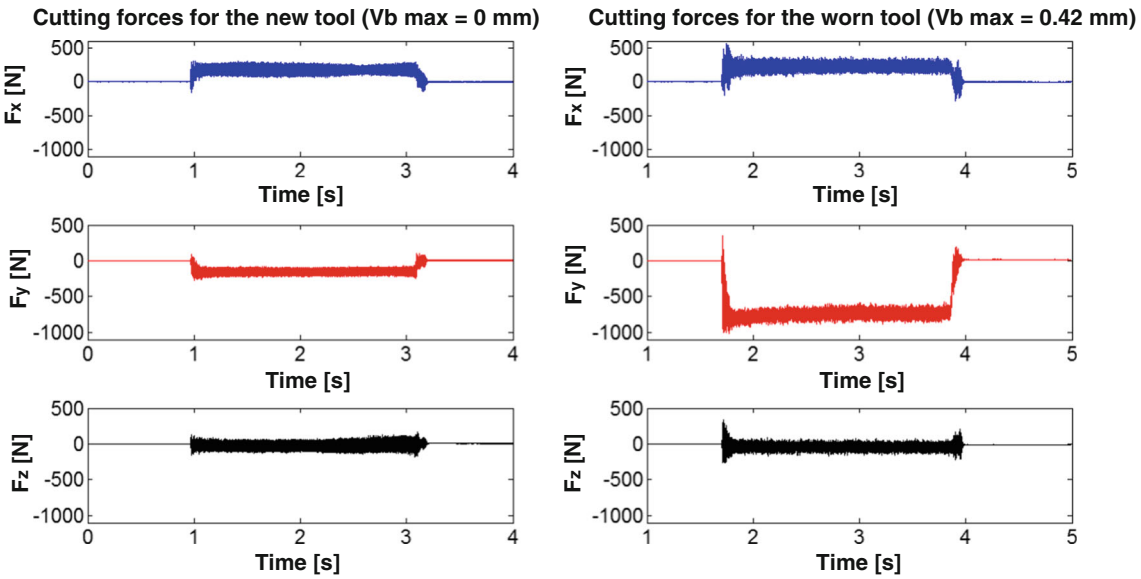

Fig. 20 Recorded forces in x-, y-, and z-directions using new and worn tools in Test 2

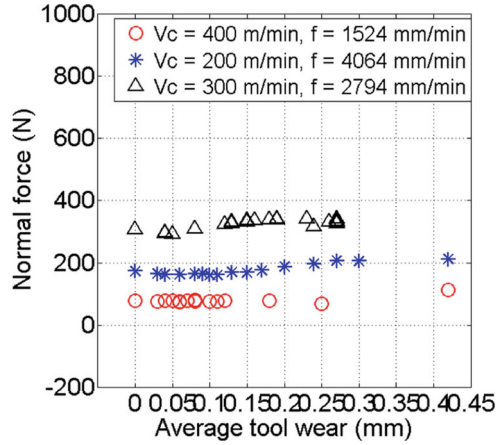

a) Normal force

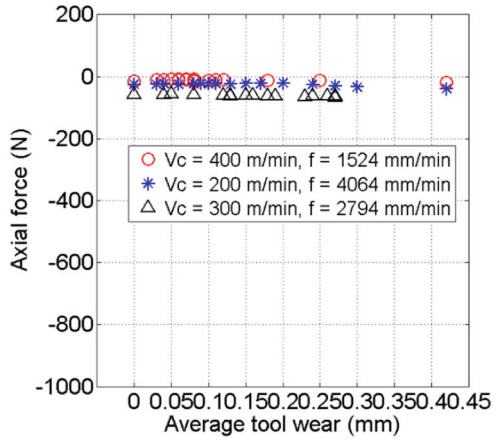

b) Axial force

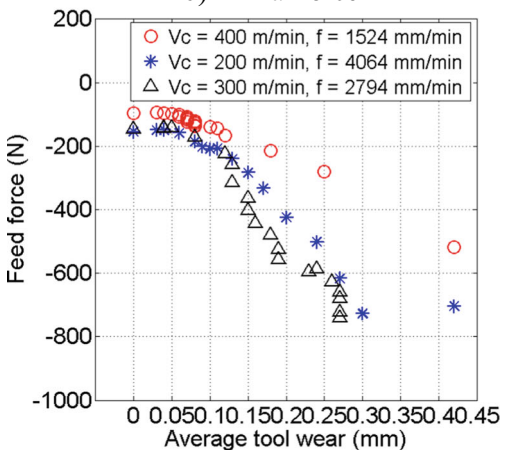

c) Feed force

Fig. 22 Cutting force components in all three tests

removed. The analysis was performed at a significance level of 5% [35].

The results presented in Table 9, show that up to eight variables are selected by our elimination test since the lowest calculated F-value =21.05> $F_{0.05,1,\ 49} = 4.03$. The percentage contribution of each variable is also calculated and presented in Table 9.

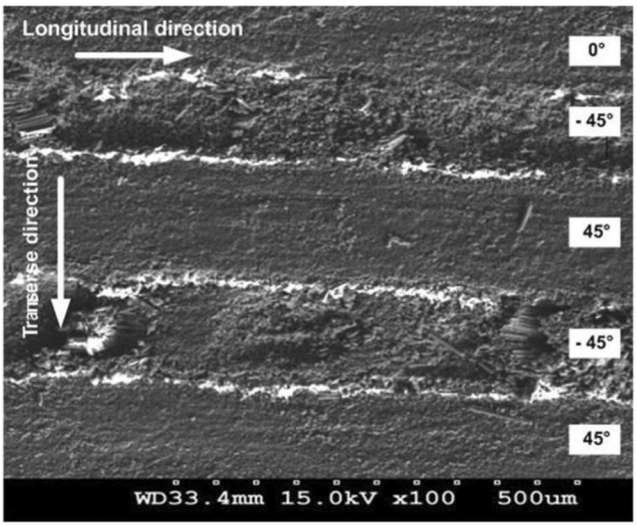

Fig. 23 Longitudinal and transverse measurement directions

The estimated model is:

$$\hat{R}_a = 9.766 - \frac{1302.614}{V_C} - \frac{7408.752}{f} - \frac{28.856}{L} + \frac{5980.616}{V_C \times L} + \frac{25903.289}{f \times L} + \frac{0.086}{L^2} - \frac{5921.321}{(V_C \times L)^2} - \frac{184700.605}{(f \times L)^2}. \quad (8)$$

The ANOVA result illustrated in Table 10 shows that $F = \frac{17.53}{0.35} = 50.08 > F_{0.05,8,\ 41} = 2.18$, which means that the model is sufficient. The calculated R-square is $R^2 = 0.91$.

As shown in Fig. 24, a very good fit was obtained.

Surface damage

It's well known that there are four types of delamination during machining of CFRP. In this work, it wasn't seen any type of delamination or fiber pull-out on the trimmed surface of all coupons for the three tool life tests (Test 1–3) using CVD coated carbide tool. This fact indicates that the high fixture rigidity, high quality of CFRP laminates, the suitable cutting tool and the stable operational conditions could decrease the fiber pull-out and delamination.

Figures 25, 26, and 27 show the SEM micrograph of the trimmed surfaces at different cutting length for Test 1–3. If we take a deepest look at material surface damage of the trimmed coupons, with an increase in tool wear, the surface quality deteriorate, meaning that matrix was burnt using worn tool due to excessive tool wear and thermal effect related to the low thermal conductivity of CFRP. On the machined surfaces which were produced using worn tool, surface damage were

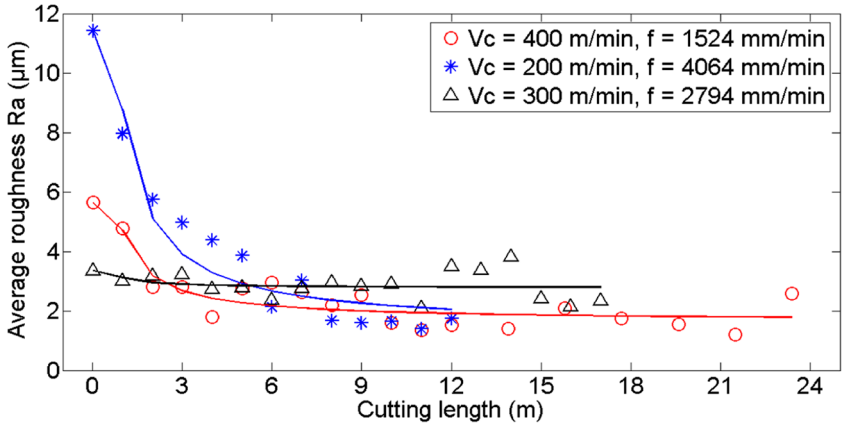

Fig. 24 Comparison of measured vs predicted values of average roughness (R_a) in all three tests

Table 9 Results of the statistical approach the roughness R_a

Significant variables	Coefficients	Standard error	F-value	Percentage; cont. %
Intercept	9.766	1.55		
$1/V_C$	−1302.614	270.42	23.20	8.97
$1/f$	−7408.752	1492.57	24.64	9.52
$1/L$	−28.856	4.94	34.16	13.20
$1/(V_C \times L)$	5980.616	834.08	51.41	19.87
$1/(f \times L)$	25,903.289	4879.11	28.18	10.89
$1/L^2$	0.086	0.02	21.05	8.14
$1/(V_C \times L)^2$	−5921.321	811.29	53.27	20.59
$1/(f \times L)^2$	−184,700.605	38,683.40	22.80	8.82

seen such as burning and thermal degradation of the CFRP matrix [36].

Similarly to the roughness results, the surface damage image shows that −45° plies represent the worst case. This is presented by matrix cracking and empty holes on the trimmed surface.

At the end of tool life tests, the excessive tool wear led to the incidence of matrix burning which was associated with smoke and acrid odor during machining. On the trimmed edges, the resin epoxy matrix was burned due to the high tool wear and high cutting force at the end of the tool life, especially in test 1 and test 2. Figure 28a shows smoke during machining using worn tool.

Figure 28b shows the burnt matrix debris at the end of the tool life in Test 2. It can be assumed that excessive tool wear and high cutting forces increased the cutting temperature. This temperature exceeded the glass transition temperature of the resin (180 °C) and consequently, it caused matrix burning/sticking and generated the acrid odor and the smoke.

Figure 29 shows the trimmed surface after 15 m of cutting length in Test 2. In this figure, it was seen that the fibers were spread and stuck. The matrix was burned due to high cutting force (737 N) and high average tool wear (0.423 mm) and it was difficult to distinguish the machined plies. For all tool life tests, same results were observed. As a solution, the use of chilled air can facilitate the removal of dust particles from the slot and decreased the incidence of matrix burning/sticking [37].

Table 10 Analysis of variance for the quadratic model (roughness R_a)

Effect	Sum of squares	D.F.	Mean squares	F-level
Regression (*SSR*)	140.26	8	17.53	50.08
Residual (*SSE*)	14.31	41	0.35	
Total (*TSS*)	154.57	49		

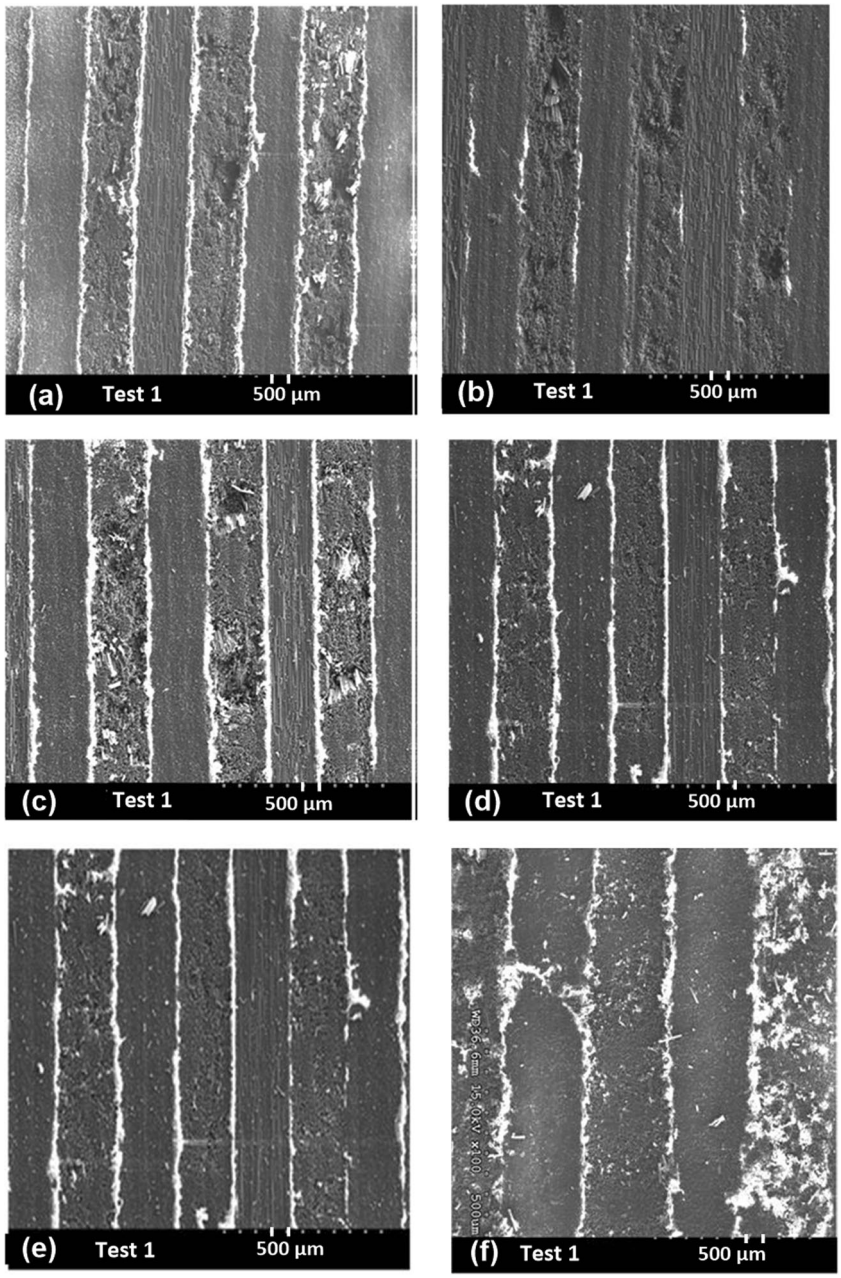

Fig. 25 SEM micrographs of trimmed surface after: **a**) 0, **b**) 4, **c**) 9, **d**) 15.8, **e**) 27.2, and **f**) 28.2 m of cut in Test 1

Conclusion and recommendation

The present work focused on the machining aspects of an autoclave-cured 24-ply CFRP laminate by using a CVD diamond-coated carbide tool with six straight flutes.

Based on the results obtained, the following conclusion can be drawn:

- From the nine preliminary tests, ANOVA shows that the feed rate is the most important factor affecting the normal and axial cutting forces. The effect of the cutting velocity is found almost negligible.
- The effect of the feed rate on the feed force is less significant than the cutting velocity. The interaction effect of the cutting velocity-feed has the highest statistical significance.
- ANOVA results of the preliminary tests show also that the interaction effect of the cutting velocity and feed rate has the highest contribution on the surface roughness.

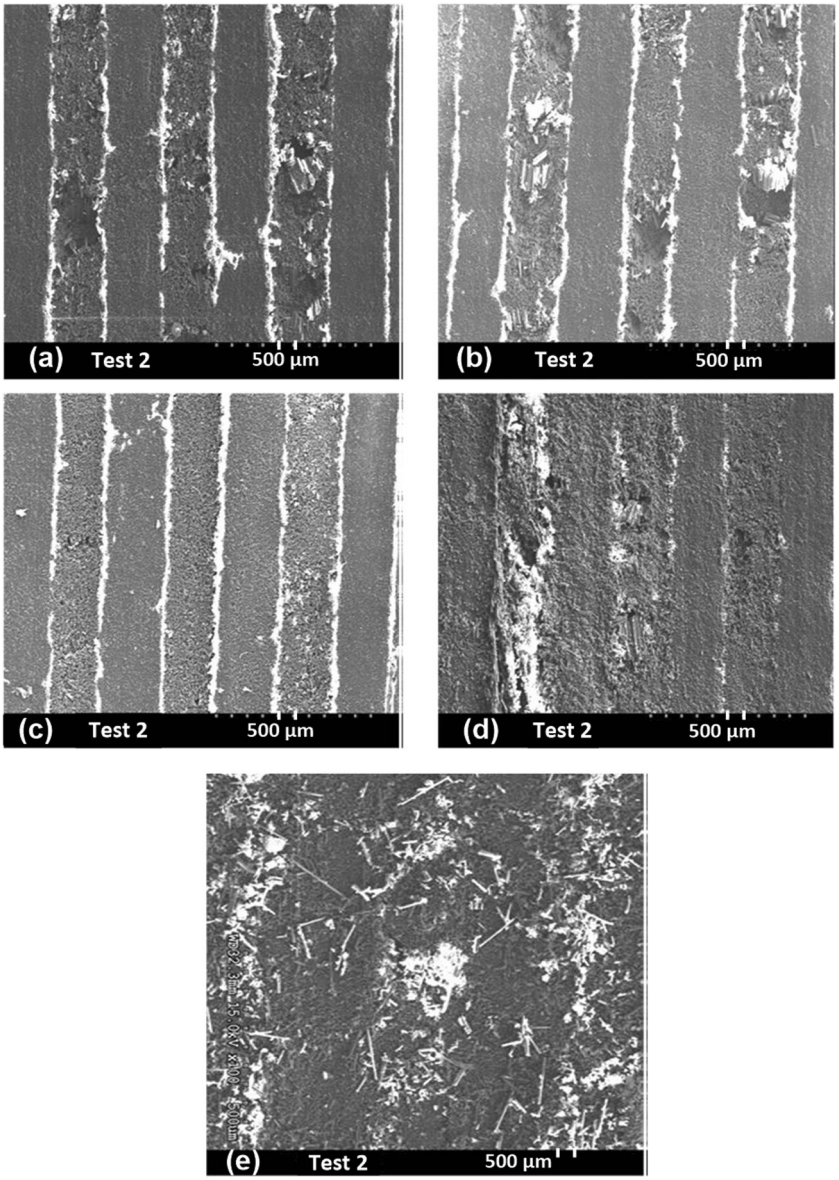

Fig. 26 SEM micrographs of trimmed surface after: **a**) 0, **b**) 4, **c**) 9, **d**) 14 and **e**) 15 m of cut in Test 2

- The developed statistical models predict successfully the cutting force components and surfaces roughness.
- During the trimming of CFRPs, the evolution of the cutting force with the cutting length is significantly affected by the flank wear of the cutting tool.
- Results showed that there is a strong correlation between the feed force and the tool wear.
- A weak correlation was observed between the normal force, the axial force and the tool wear.
- ANOVA results proved that the proposed reciprocal model demonstrates a high capacity to accurately predict surface roughness under the conditions studied.
- The −45° ply orientation leads to poor surface roughness and high surface damage, presented by matrix cracking and empty holes on the trimmed surface.
- When the tool wear increased the temperature at the cutting zone increased and this leads to surface damage meaning that matrix was burnt using worn tool.
- The 0° ply orientation produced the maximum tool wear. However, further work is certainly required to reinforce

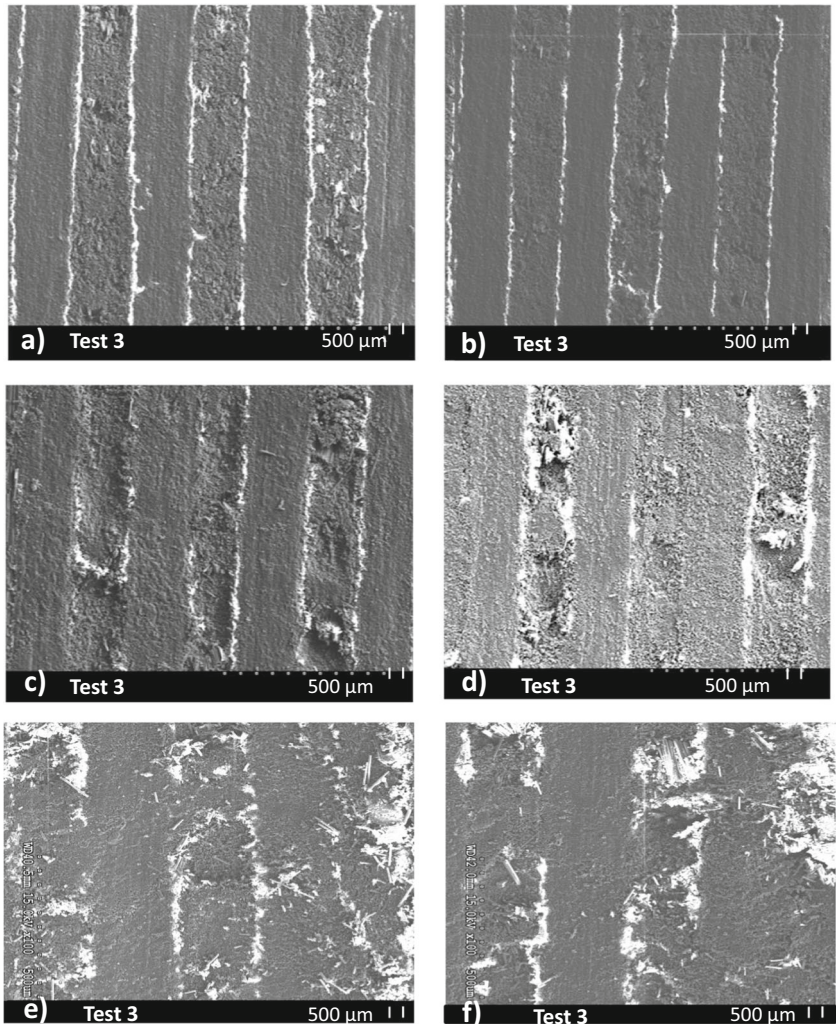

Fig. 27 SEM micrographs of trimmed surface after: **a**) 0, **b**) 4, **c**) 9, **d**) 14, **e**) 19 and **f**) 20 m of cut in Test 3

this conclusion and different CFRP laminates with a different configuration (not 0° in the middle) needs to be used in the future experiments.

– The surface roughness decreased with an increase in the cutting length, this means that an increase in the tool wear leads to an improvement of the surface roughness, which is not a logical behavior in machining process and goes against the effect of tool wear. Briefly, if tool wear is present, R_a becomes inappropriate indicator for roughness evaluation.

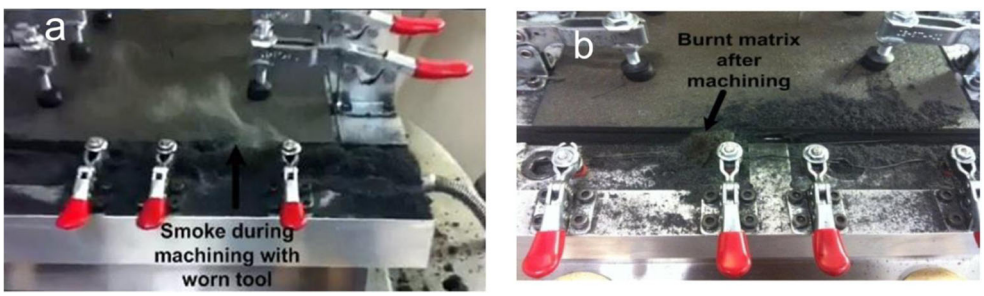

Fig. 28 Behavior of CFRP during machining, **a**) Smoke from burnt matrix in Test 2, **b**) Burnt matrix in Test 2

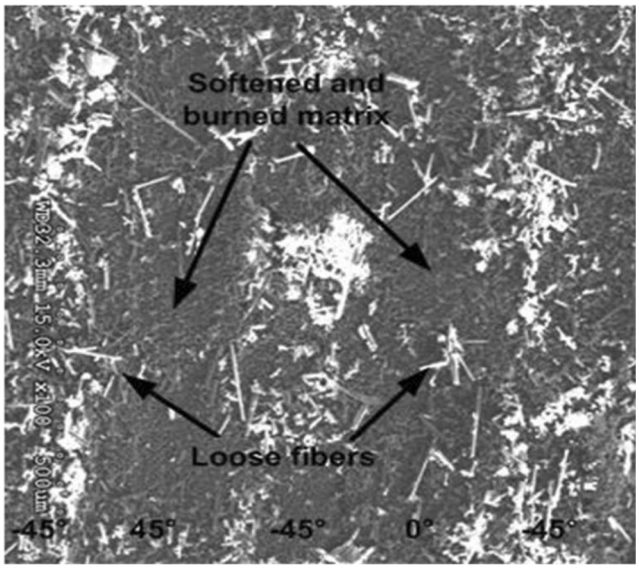

Fig. 29 Trimmed surface after 15 m of cutting length (Average VBmax = 0.42 mm) in Test 2

Funding This study was funded by the Natural Sciences and Engineering Research Council of Canada (grant number 217168–2012).

Compliance with ethical standards

Conflict of interest The authors declare that they have no conflict of interest.

Publisher's Note Springer Nature remains neutral with regard to jurisdictional claims in published maps and institutional affiliations.

References

1. Davim JP (2010) Machining Composite Materials. John Wiley & Sons Inc., London, England
2. Sheikh-Ahmad JY (2009) Machining of polymer composites. Springer, New York
3. Everstine G, Rogers T (1971) A theory of chip formation of FRP composite materials. Journal of Comput Mater Sci 5(1):94–106
4. Koplev A (1980) Cutting of CFRP with single edge tools. Proceedings of the third international conference on composite materials 2, Paris, France 1597–605
5. Roudgé M, Cherif M, Cahuc O, Darnis P, Danis M (2008) Multilayer Materials Qualitative Approach of the Process. Int J Mater Form 1(S1):949–952
6. Caggiano A (2018) Machining of Fibre Reinforced Plastic Composite Materials, materials, doi:https://doi.org/10.3390/ma11030442
7. Sheikh-Ahmad J, Twomey J, Kalla D, Lodhia P (2007) Multiple regression and committee neural network Force prediction models in milling FRP. Mach Sci Technol 11:391–412
8. Koplev A, Lystrup A, Vorm T (1983) The cutting process, chips and cutting forces in machining CFRP. Composites 14(4):371–376
9. Slamani M, Gauthier S, Chatelain J-F (2015) A study of the combined effects of machining parameters on cutting force components during high speed robotic trimming of CFRPs. Measurement 59:268–283
10. Arola D, Ramulu M (1997) Orthogonal cutting of fiber-reinforced composites: A finite element analysis. IJMS 39(5):597–613
11. Chatelain J-F, Zaghbani I (2012) A Comparison of Special Helical Cutter Geometries Based on Cutting Forces for the Trimming of CFRP Laminates. International Journal of Mechanics 6(1):52–59
12. Rimpault X, Chatelain J-F, Klemberg-Sapieha JE, Balazinski M (2017) Tool wear and surface quality assessment of CFRP trimming using fractal analyses of the cutting force signals. CIRP-JMST 16:72–80
13. Haiyan W, Xuda Q, Hao L, Chengzu R (2012) Analysis of cutting forces in helical milling of carbon fiber-reinforced plastics. Proc Inst Mech Eng B JEng Manuf 227(1):62–74
14. Boudelier A, Ritou M, Garnier S, Furet B (2018) Cutting force model for machining of CFRP laminate with diamond abrasive cutter. Prod Eng 12(2). https://doi.org/10.1007/s11740-018-0813-4
15. Slamani M, Chatelain J-F, Hamedanianpour H (2015) Comparison of two models for predicting tool wear and cutting force components during high speed trimming of CFRP. Int J Mater Form 8(2):305–316
16. Xu W, Zhang L (2018) Tool wear and its effect on the surface integrity in the machining of fibre-reinforced polymer composites. Compos Struct 188. https://doi.org/10.1016/j.compstruct.2018.01.018
17. Kerrigan K, O'Donnell GE (2016) On the relationship between cutting temperature and workpiece polymer degradation during CFRP edge trimming. Procedia CIRP 55:170–175
18. Ghidossi P, El-Mansori M, Pierron F (2004) Edge machining effects on the failure of polymer matrix composite coupons. Composites Part A 35(7–8):989–999
19. Rajasekaran T, Vinayagam BK, Palanikumar K, Prakash S (2010) Influence of machining parameters on surface roughness and material removal rate in machining carbon fiber reinforced polymer material. Frontiers in Automobile and Mechanical Engineering (FAME) 1:75–80
20. Arola D, Ramulu M, Wang DH (1996) Chip formation in orthogonal trimming of graphite/epoxy composite. Composites Part A 27(2):121–133
21. Wang XM, Zhang LC (2003) An experimental investigation into the orthogonal cutting of unidirectional fibre reinforced plastics. Int J Mach Tools Manuf 43(10):1015–1022
22. Wang C, Ming W, An Q, Chen M (2017) Machinability characteristics evolution of CFRP in a continuum of fiber orientation angles. Mater Manuf Process 32(9):1041–1050
23. Hintzea W, Brügmanna F (2018) Influence of spatial tool inclination on delamination when milling CFRP. J Mater Process Technol 252:830–837
24. Su F, Yuan J, Sun F, Wang Z, Deng Z (2018) Analytical cutting model for a single fiber to investigate the occurrences of the surface damages in milling of CFRP. Int J Adv Manuf Technol 96(5-8). https://doi.org/10.1007/s00170-018-1797-0
25. Gilpin A (2009) Tool solutions for machining composites. Reinf Plast 53(6):30–33
26. ISO Standard 8688–2 (1989) International standard for tool life testing in end milling, part 2, 1st edn, 1989-05-01.
27. Zaghbani I, Chatelain J-F, Songmene V, Berube S, Atarsia A (2012) A comprehensive analysis of cutting forces during routing of multilayer carbon fiber-reinforced polymer laminates. J Compos Mater 46(16):1955–1971
28. Slamani M, Gauthier S, Chatelain J-F (2016) Comparison of surface roughness quality obtained by high speed CNC trimming and high speed robotic trimming for CFRP laminate. Robot Comput Integr Manuf 42:63–72

29. Berube S (2012) Évaluation de la performance d'outils de coupe dédiés au détourage de structures composites carbone/époxy. Master dissertation, École de technologie supérieure de Montréal, Canada
30. Sheikh-Ahmad JY, Urban N, Cheraghi H (2012) Machining Damage in Edge Trimming of CFRP. Mater Manuf Process 27(7):802–808
31. ASME (2009) ANSI B46.1: Surface Texture (Surface Roughness, Waviness, and Lay). ASME, New York, NY, USA
32. Duboust N, Ghadbeigi H, Pinna C, Ayvar-Soberanis S, Collis A, Scaife R, Kerrigan K (2017) An optical method for measuring surface roughness of machined carbon fibre-reinforced plastic composites. J Compos Mater 51(3):289–302
33. Eneyew ED, Ramulu M (2014) Experimental study of surface quality and damage when drilling unidirectional CFRP composites. Journal of Materials Research and Technology 3(4):354–362
34. Trefethen LN, Bau D (1997) Numerical Linear Algebra. SIAM, Philadelphia
35. Mason RL, Gunst RF, Hess J-L (2003) Statistical design and analysis of experiments, with applications to engineering and science. John Wiley & Sons, Inc., Hoboken
36. Hamedanianpour H, Chatelain JF (2013) Effect of Tool Wear on Quality of Carbon Fiber Reinforced Polymer Laminate during Edge Trimming. Appl Mech Mater 325–326:34–39
37. El-Hofy MH, Soo SL, Aspinwall DK, Sim WM (2011) Pearson D, Harden P. Factors Affecting Workpiece Surface Integrity in Slotting of CFRP. Procedia Engineering 19:94–99